RESEARCH ARTICLE OPEN ACCESS

# DR-FEDPAM: Detection of Diabetic Retinopathy using Federated Proximal Averaging Model

Gaya Nair Po, and Lanitha Bo

Department of Computer Science and Engineering, Karpagam Academy of Higher Education, Coimbatore, Tamil Nadu, India.

**Corresponding author**: Lanitha B. (e-mail: lanithanandakumar@gmail.com), **Author(s) Email**: Gaya Nair P (gsgayasajeev@gmail.com)

Abstract. Diabetic retinopathy (DR) is an eye condition caused by damage to the blood vessels of the retina due to high blood sugar levels, commonly associated with diabetes. Without proper treatment, it can lead to visual impairment or blindness. Traditional machine learning (ML) approaches for detecting Diabetic retinopathy rely on centralized data aggregation, which raises significant privacy concerns and often encounters regulatory challenges. To address these issues, the DR-FEDPAM model is proposed for the detection of diabetic retinopathy. Initially, the images are preprocessed using a Median Filter (MeF) and Gaussian Star Filter (GaSF) to reduce noise and enhance image quality. The preprocessed images are then input into a federated proximal model. Federated Learning (FL) enables multiple local models to train on distributed devices without sharing raw data. After the local models process the data, their parameters are aggregated through a Global Federated Averaging (GFA) model. This global model combines the parameters from all local models to produce a unified model that classifies each image as either normal or diabetic retinopathy. The model's performance is evaluated using precision (PR), F1-score (F1), specificity (SP), recall (RE), and accuracy (AC). The DR-FEDPAM achieves a balanced trade-off with 7.8 million parameters, 1.7 FLOPs, and an average inference time of 13.9 ms. The model improves overall accuracy by 5.44%, 1.89%, and 4.43% compared to AlexNet, ResNet, and APSO, respectively. Experimental results show that the proposed method achieves an accuracy of 98.36% in detecting DR.

Keywords Diabetic retinopathy; Retinal image; Median Filter; Gaussian Star Filter; Federated Learning; MobileNet; Global Federated Averaging Model

#### I. Introduction

Diabetic retinopathy (DR) is a severe microvascular complication of diabetes mellitus that damages the retinal blood vessels, leading to vision impairment and, in advanced stages, blindness [1], [2]. The disease progression is categorized into non-proliferative DR (NPDR) and proliferative DR (PDR), both of which can cause irreversible vision loss if not detected early [3], [4]. The global burden of diabetes is increasing at an alarming rate, and consequently, DR prevalence is expected to reach unprecedented levels [5]. Delayed detection remains a critical issue because early symptoms are often subtle, requiring advanced image analysis techniques for accurate diagnosis [6]. Deep learning (DL) [7] and machine learning (ML) [8] methods, particularly convolutional neural networks (CNNs) [9], have shown strong performance in automated DR detection from retinal fundus images [10]. Various architectures such as ResNet [11], AlexNet [12], RegNet [13], and GoogleNet [14] have been used for feature extraction and classification. Some approaches integrate lesion detection, attention mechanisms, or hybrid feature selection strategies. achieving moderate to high accuracy [15]. Moreover, federated learning (FL) has emerged as a promising paradigm for collaboratively training models without centralizing sensitive medical data, thereby enhancing privacy preservation [16].

Despite these advancements, existing DR detection methods still face challenges such as generalization computational complexity. limited across datasets, dependency on large labeled datasets, and data privacy concerns in centralized training [17]. Many models require substantial hardware resources, which hinders real-time clinical particularly in resource-constrained deployment, environments [18]. Furthermore, privacy regulations restrict the direct sharing of patient images, making centralized learning models less feasible in real-world medical scenarios [19]. To address these limitations, this study proposes DR-FEDPAM (Detection of Diabetic Retinopathy using Federated Proximal Averaging Model). The proposed approach begins with image preprocessing using the Median Filter (MeF) and Gaussian Star Filter (GaSF) to reduce noise and enhance image quality. A federated proximal learning framework is then employed, where multiple clients train local MobileNet-based models without sharing raw

data. The server aggregates the local model parameters using a Global Federated Averaging (GFA) strategy to create an optimized global model that classifies retinal images into Normal or DR categories.

The main objective of this study is to develop a high-accuracy, privacy-preserving, and computationally efficient deep learning model for early detection of diabetic retinopathy using federated learning, enabling robust performance without compromising patient data confidentiality. The key contributions of this model are summarized as follows:

- Input retinal images undergo preprocessing steps, including the GaSF and MeF, to eliminate noise and improve image quality.
- The enhanced image are fed into a Federated Proximal Model. FL enables multiple local models to train on different devices without sharing raw data.
- After the local models process the data, their parameters are aggregated using the GFA Model. This model combines parameters from all local models to create a global model that classifies images as either Normal or DR.
- 4. The efficiency of the proposed DR-FEDPAM model is evaluated/assessed based on F1-score (F1), recall (RE), specificity (SP), precision (PR), and accuracy (AC).

The structure of this paper (study) is organized as follows: Section 2 briefly describes the literature survey; Section 3 presents the proposed DR-FEDPAM model; Section 4 discusses the performance results and comparative analysis; and Section 5 concludes with remarks and future work.

#### **II.** Literature Survey

In recent years, several studies have investigated the classification of DR detection using deep neural networks and ML methods. The section that follows provides a review of some recent research works.

In 2022 Lahmar, C. and Idri, A., [20] proposed CNN and ML models for DR classification. The hybrid architecture combining MobileNetV2 and an SVM classifier for feature extraction achieved the best performance and was classified as one of the most effective end-to-end DL architectures, with an accuracy of 88.80%. Dasari, S., et al. [21] developed an efficient ML-based technique for DR identification in 2023. This study described an effective system-based DR classification method. To detect DR spontaneously and accurately, the efficient ML-DRGC design was proposed for ML-based grading classification. A DLbased method for DR was introduced by Fayyaz, A.M. et al [22] in 2023. This method utilized DL to enhance the performance of computer-aided diagnosis for DR. The system was designed for portable diagnostic equipment and incorporated CNN and ResNet architectures, as suggested by Basheer, S. and Varghese, R.E., [23] in 2024.

DL with optimized feature selection was proposed by Sapra et al. [24] in 2024 for DR detection. The proposed DL model achieved 93.5% accuracy (AC) with an optimized feature subset. Based on lesion features, Jabbar et al [25] developed a DL model for DR detection. Experimental results demonstrated that the proposed hybrid model/framework outperformed advanced techniques on the benchmark dataset, achieving 94% accuracy. To detect DR, Chaudhuri, R and Deb, S., proposed Mask-RCNN and Generative Adversarial Networks [26]. The objective of this study was to diagnose DR by analyzing fundus images using DL techniques. In 2024, Mutawa et al. [27] outlined a DL model for detecting DR stages. This study made a significant contribution to understanding DR by employing two distinct public datasets. The CNN architecture was fine-tuned using various learning rates and optimizers.

Based on the above literature survey, various DL and ML approaches have been developed for DR detection. However, these methods exhibit low reliability due to factors such as high time complexity and limited image datasets. To address these challenges, the DR-FEDPAM model has been proposed for more effective DR detection.

#### III. Proposed System

In this section, the DR-FEDPAM model is proposed for DR detection. The proposed DR-FEDPAM model is illustrated in Fig. 1. The DR-FEDPAM workflow begins by dividing the DDR dataset among 20 clients with non-IID data distributions. Each client performs local training on its dataset using the MobileNet model for one epoch. After training, only the model weights are transmitted to the central server, thereby preserving data privacy. The server aggregates these updates using the Federated Averaging algorithm. This process is repeated for 100 communication rounds. The final global model is then used to classify retinal images as either Normal or DR.

# A. Dataset description

The DDR dataset [28] contains 13,673 fundus images, comprising 6835 training images, 4105 test images, and 2733 validation images acquired at a 45° field of view for DR grading and lesion segmentation. The data were collected from 147 hospitals across 23 regions in China and annotated by a professional team using the International Classification of Diseases and Risks scale. Several qualified graders categorized the photographs into six classes. The dataset includes 1151 non-gradable images, 6266 normal images, and 6256 DR images. A total of 757 images were pixel-

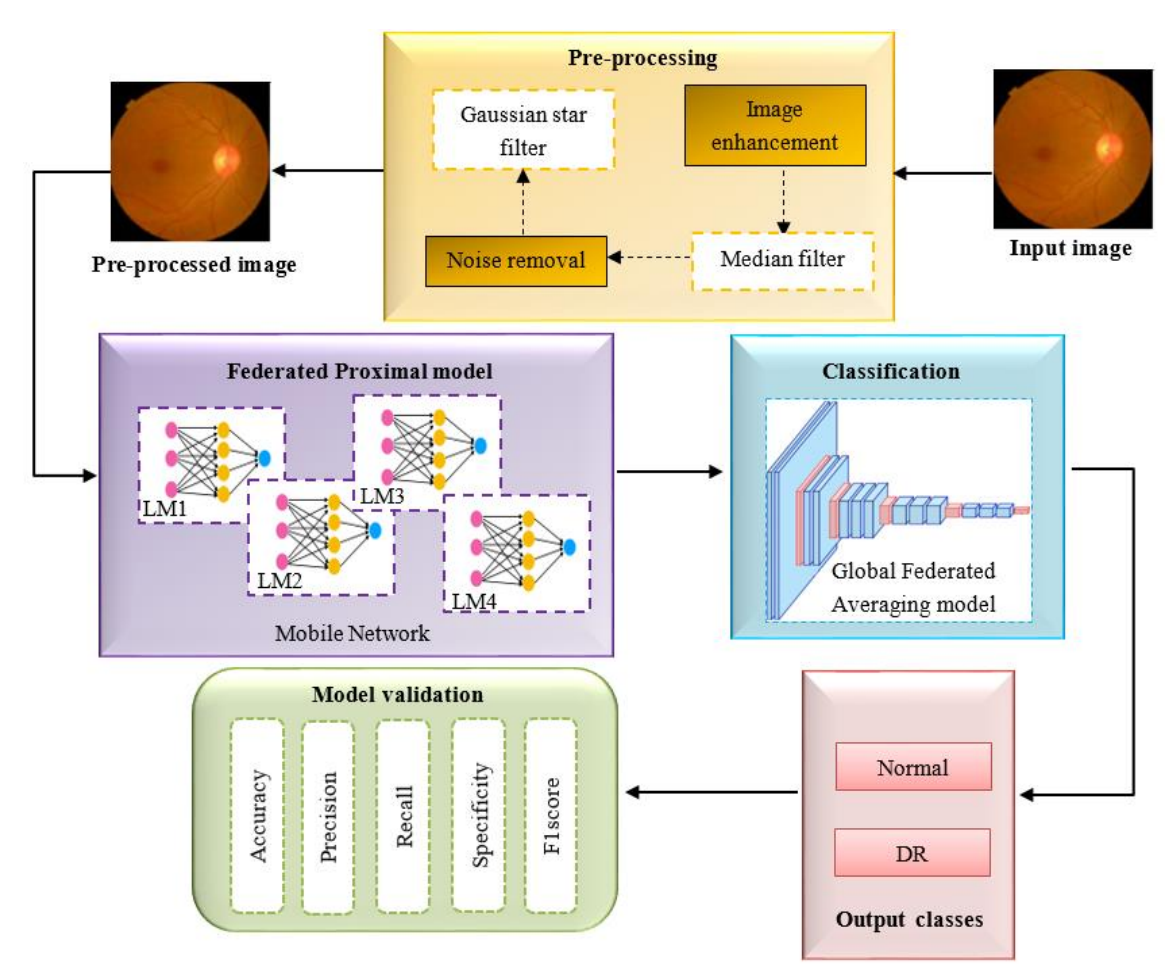


Fig. 1. Proposed DR-FEDPAM model

labeled with bounding boxes to assist in lesion detection and segmentation.

#### B. Data preprocessing

Preprocessing enhances medical images by eliminating noise and improving subtle visual variations. The Median Filter (MeF) is applied to enhance image quality, while the Gaussian Star Filter (GaSF) is used to suppress noise in the images.

#### Median filter

In this stage, the MeF [29] is applied to improve image quality and is particularly effective at reducing salt-and-pepper noise, which occurs when certain pixels have extremely high or low intensity values compared to their surroundings. In this method, surrounding pixels are ranked by brightness, and the median value is assigned as the new intensity for the central pixel. Unlike conventional smoothing filters that blur edges, the median filter preserves boundaries effectively. The kernel is less sensitive to outliers, allowing unwanted artifacts to be removed more efficiently. Because the edges are only slightly degraded, the MeF can be applied multiple times if necessary. Digitization artifacts, such as straight lines that appear in

mammographic images, can be addressed using a two-dimensional (2D) median filtering approach for a  $3\times3$  neighborhood window. The primary drawback of MeF is that it generates a new flag point that does not exist in the original flag, which may be problematic in certain applications. The MeF removes both noise and fine details. Features smaller than the neighborhood size have minimal effect on the median value and are therefore filtered out. Thus, the MeF cannot distinguish fine details from noise. Given an image I of size M×N times: let (x, y) denote the coordinates of the pixel being processed. Consider a neighborhood  $W_{x,y}$  around the pixel I (x, y) of size m×n. The MeF output for the pixel I'(x,y) is defined in (Eq. (1)): [30]

$$I'(x,y) = median \left\{ I(x+k,y+l) | k = -\frac{m-1}{2}, \dots \right\}$$
 (1)

Where, I (x+k, y+l) denotes the pixel values within the window centered on (x, y). With k and I representing the horizontal and vertical offsets, respectively. The median value corresponds to the middle value when all pixels in  $W_{x,y}$  are arranged in ascending order.

#### 2. Gaussian star filter

In this stage, the GaSF [31] is used for noise suppression, image smoothing, and nonlinear edge shaping in the input image. The proposed filter consists of two orthogonal Gaussian filters with elliptic profiles, each forming a star-shaped filter for every noise peak. Based on image amplitude, a region-growing technique is employed to estimate the filter parameters for each noise peak.

The Fourier amplitude spectrum of periodic and quasi-periodic noise typically exhibits a star-like pattern, which motivates the star-shaped filter design. The GaSF applies linear smoothing using a 3×3 average filter. The square region is identified as an unclassified low-frequency zone using the GaSF method. Manual threshold values are applied for parameter control. The Gaussian function is defined in Eq. (2): [32]

$$G(x,y) = \frac{1}{2\pi\sigma^2} exp\left(-\frac{x^2 + y^2}{2\sigma^2}\right)$$
 (2)

where x and y represent the horizontal and vertical axes, and G(x,y) denotes the Gaussian kernel value at coordinates (x,y).  $\sigma$  represents the standard deviation of a Gaussian distribution, while  $2\pi\sigma^2$  defines the normalization factor ensuring that the total volume under the Gaussian function equals 1. Consequently,  $\sigma$  determines the amount of blurring produced by the Gaussian kernel.

Table 1. Parameter for pre-processing filter

	· · ·	•
Filter	Parameter	Value
MeF and GaSF	Kernel Size	3×3
GaSF	Sigma (σ)	1.5
GaSF	Manual Threshold	0.25
GaSF	Elliptic Filter Radius	2

Table 1 presents the parameter settings used in the pre-processing stage of the DR-FEDPAM model. The MeF applies a  $3\times3$  kernel to eliminate salt-and-pepper noise while preserving edge details. The GaSF also uses a  $3\times3$  kernel and is configured with a  $\sigma$  of 1.5 to control smoothing intensity. A manual threshold of 0.25 and an elliptic radius of 2 enable precise suppression of periodic noise peaks in retinal images.

#### A. Federated Proximal Model

Eq. (4) [33] illustrates the usual convolutional layer's computing cost.

$$Q_r = H_{o_{/p}} \times H_{o/p} \times i \times l \times H_{i_p} \times H_{i_p}$$
 (4)

Where,  $\mathcal{Q}_r$  denotes the Computational cost of a conventional convolution layer and  $\mathrm{H}_{o/p}$  denotes height of the output feature map. I denote number of input

The preprocessed image is fed into the Federated Proximal (FedProx) model. Federated learning enables multiple local models to train on different devices without sharing raw data. Each local model processes its data independently on the respective device. MobileNet, developed by a Google research team, employs convolutional layers that are separable by depth. The ideal weighted model refers to a pretrained MobileNet initialized with weights obtained from prior training on the DDR dataset. This model is not trained from scratch at the client level but is loaded for feature extraction. Channel-wise and spatial features are extracted from retinal images using MobileNet's depthwise separable convolutions. These features assist in detecting DR-related patterns locally. The use of pretrained weights enhances convergence speed and reduces training overhead at each client. All model updates are performed using local data, and the global model is constructed through federated averaging. This approach ensures computational efficiency and privacy preservation while maintaining high classification performance. The architecture of MobileNet is shown in Fig. 2.

Furthermore, with only a few hyperparameters, the MobileNet architecture achieves high accuracy. The depthwise separable convolution layers represent the cross-channel and spatial correlations detected in the input image feature maps. To operate, a depthwise separable convolution performs two types of convolutions: pointwise and depthwise. The pointwise convolution (1×1) applies a filter to identify crosschannel patterns, whereas the depthwise convolution (DWC) employs a single spatial filter for each input feature map. Standard convolutional layers extract both cross-channel and spatial patterns simultaneously, whereas separable convolutional layers process them independently. The integration of deep and separable convolutional networks accelerates MobileNet training and significantly reduces overall computational cost. The standard convolutional structure is mathematically defined in Eq. (3) [33]:

$$\Re_r = \sum_i \omega_{i,l} \cdot I_i \tag{3}$$

where  $\Re_r$  represents the Output feature representation at layer r and  $\omega_{i,l}$  defines the Learnable weights (convolutional filter parameters) for input channel i at layer l.  $\mathrm{I}_i$  represents the input feature map from the i-th channel, while  $\sum i$  denotes the summation over all input channels i.

channels and I denote number of output channels.  $H_{in}$  represents the Kernel size.

Eq. (5) [33] illustrates the DWC stage. where  $I_k$  indicates the input data and  $\wp_{1,i}$  represents the kernels.

$$\chi_i = \sum \wp_{1,i} \cdot I_i \tag{5}$$

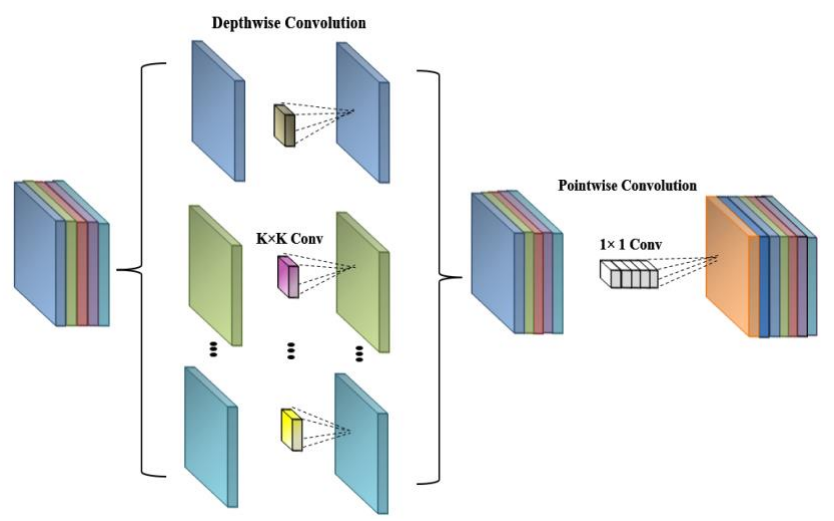


Fig. 2. Architecture of MobileNet

where,  $\chi_i$  represents the output of the depthwise convolution for input channel I and  $\wp_{1,i}$  represents the depthwise convolution kernel applied only to the i-th input channel. A  $\mathrm{H}_{o/p} \times \mathrm{H}_{o/p}$  length and k filters with I channels are provided for DWC. Eq. (6) [33] is used to determine the computing cost of the extensive separable convolution structure.

$$\mathcal{F}_{\nu} = H_{o/p} \times H_{o/p} \times k \times H_{i_p} \times H_{i_p} + k \times l \times H_{i_p} \times H_{i_p}$$
 (6)

Where,  $\mathcal{F}_{\nu}$  denotes the computational cost of depthwise separable convolution and  $\mathrm{H}_{o/p}$  defines the Output feature map size. k denotes number of filters applied in the depthwise convolution stage, I Number of output channels after pointwise convolution and  $\mathrm{H}_{i_p}$  denotes the Kernel size. The cost of the suggested technique is  $\frac{1}{l} + \frac{1}{\mathrm{H}^2_{o/p}}$  when comparing the above

computational cost equation with the conventional convolutional method. By using deep and separable convolutional structures, MobileNet enables rapid training and fewer computations.

Table 2 outlines the key hyperparameters and regularization settings used to train the MobileNet model in the proposed DR-FEDPAM model. Each local

**Table 2. Training Parameters of MobileNet** 

Value		
1		
0.001		
AO		
0.3		
32		
Categorical Cross-Entropy		
$L2 (\lambda = 0.0001)$		
Patience = 10 rounds		

client trains for one epoch per communication round to maintain computational efficiency. A learning rate of 0.001 ensures stable convergence, while a batch size of 32 balances performance and memory usage. The Adam optimizer (AO) is selected for its adaptive learning capability. Dropout is applied to reduce overfitting, and L2 regularization ( $\lambda$  = 0.0001) is employed to penalize large weights. Early stopping with a patience of 10 communication rounds is implemented to prevent unnecessary training when validation performance plateaus.

## **B.** Global Federated Averaging Model

After the local models process the data, the results are combined using the Global Federated Averaging (GFA) model. In this model, all local parameters are aggregated to create a global model, which is then used to classify images as Normal or DR. In DR-FEDPAM model, federated learning involves 20 local clients with non-independent and identically (non-IID) data. For each training round, 10 clients are randomly selected to participate. Each client trains the model locally for one epoch. The local updates are sent to a central server for aggregation using the Federated Averaging algorithm. Client selection is performed using uniform random sampling without replacement. This process continues for 100 global communication rounds to construct the final global model. In the outermost loop, a global learning cycle is iterated a predetermined number of times. During each iteration, the system sets global parameters. The client-side feature extraction process involves loading a pretrained model from the retinal image dataset, randomly splitting the data into packets for prediction, packaging the data as  $FE_x$  and transmitting it to the edge server. The edge server performs two main processes: the first is global edge communication training, followed by extraction and linking of local features from client data. The model is then weighted in conjunction with the overall global

Manuscript received May 12, 2025; Revised August 20, 2025; Accepted September 10, 2025; date of publication October 16, 2025 Digital Object Identifier (**DOI**): https://doi.org/10.35882/jeeemi.v7i4.915

Copyright © 2025 by the authors. This work is an open-access article and licensed under a Creative Commons Attribution-ShareAlike 4.0 International License (CC BY-SA 4.0).

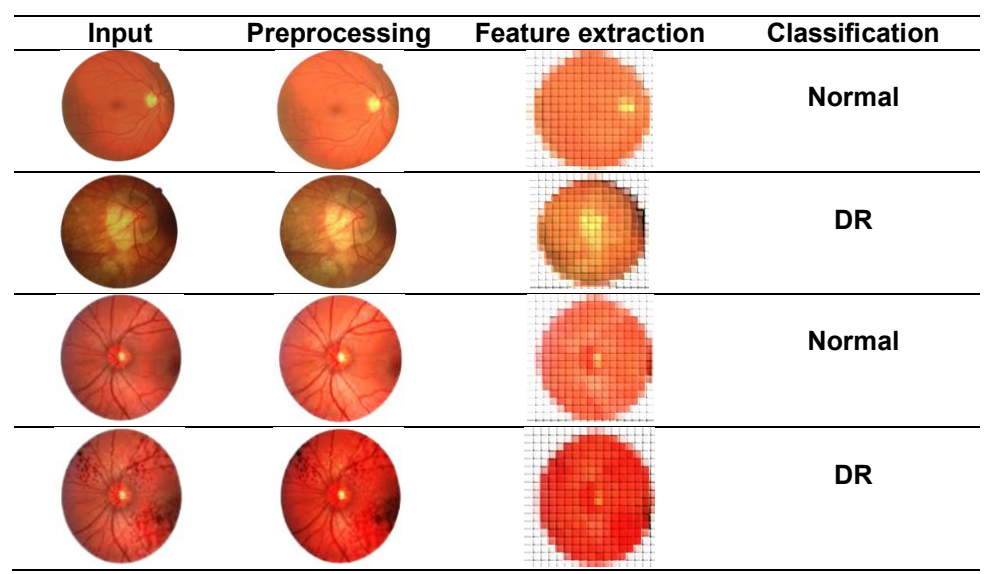


Fig. 3. Classification results of proposed DR-FEDPAM model

model. The client utilizes the DDR dataset to update the pretrained data, after which the extracted data are reconnected. The edge server subsequently trains on the full dataset to generate local weights. The algorithm can send a predetermined round-robin schedule to the edge-sever based on the assigned weight  $w_0$ . After the training stage, the edge server weight is adjusted during communication loops. Upon collecting the weight lists from all contributing edges, the model combines and averages them. The weights are adjusted again for the next round. Following local training, the server receives the models from all participating clients. The global model  $w^{(i+1)}$  at round i+1 is obtained by averaging the weights of all local models, weighted by the number of data points  $|D_k|$  for each client, as defined in Eq. (7) [34]:

$$w^{(i+1)} = \sum_{k=1}^{K} \frac{|D_k|}{\sum_{j=1}^{K} |D_j|} w_k^{(i+1)}$$
 (7)

Where,  $w^{(i+1)}$  is the global model after round i+1,  $|D_k|$  is the number of data points on client k and  $w_k^{(i+1)}$  is the local model for client k after round i+1 K is the number is contributing clients. The classification model is trained to identify whether the retinal image indicates Normal or DR.

## IV. Result

This section presents the evaluation of the proposed DR-FEDPAM model using the collected dataset, applying several performance metrics including precision (PR), recall (RE), specificity (SP), accuracy (AC), and F1 score. The benchmark includes the performance of the proposed model as well as the overall accuracy rate, which has been clearly defined and evaluated. Fig. 3 presents the classification results of the proposed DR-FEDPAM model using the DDR

dataset. Column 1 shows the input image, and Column 2 displays the preprocessed image. Column 3 presents the feature-extracted image, and Column 4 represents the final classification output.

# A. Performance analysis

The proposed DR-FEDPAM model is evaluated based on specificity (SP), precision (PR), recall (RE), accuracy (AC), and F1 score. Specificity measures the model's accuracy in identifying negative cases. It is computed by dividing the total number of negatives by the number of correctly predicted negatives, as defined in Eq. (8) [35]:

$$SP = \frac{T_{neg}}{T_{neg} + F_{pos}} \tag{8}$$

PR calculates the percentage of optimistic forecasts that come true. It emphasizes the model's ability to minimize false positives in Eq. (9) [35]:

$$PR = \frac{T_{pos}}{T_{nos} + F_{nos}} \tag{9}$$

RE evaluates the model's capacity to accurately detect every real positive case. It is the ratio of correctly predicted positive observations to all actual positives in Eq. (10) [35]:

$$RE = \frac{T_{pos}}{T_{pos} + F_{neg}} \tag{10}$$

AC calculates how accurate the model's predictions are overall. It is computed as the proportion of accurately predicted samples to all samples in Eq. (11) [35]:

$$AC = \frac{T_{pos} + T_{neg}}{Total\ no.of\ samples} \tag{11}$$

F1 represents the harmonic mean of PR and RE, offering a balanced measure when there is an uneven class distribution in Eq. (12) [35]:

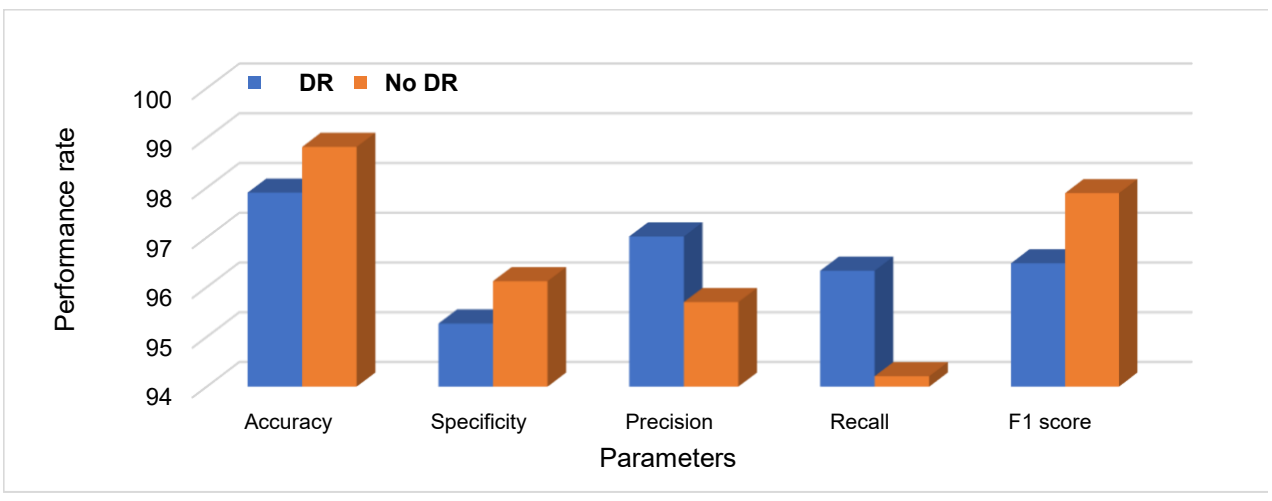


Fig. 4. Graphical representation of performance analysis

$$F1 = 2\left(\frac{PR + RE}{PR + RE}\right) \tag{12}$$

In Eq. (8), Eq. (9), Eq. (10), Eq. (11) and Eq. (12) [35],  $T_{neg}$  and  $T_{pos}$  specifies true negatives and true positives of the sample images,  $F_{neg}$  and  $F_{pos}$  requires false negatives and false positives of the sample images. High AC reflects the overall correctness of the model's predictions across all cases. High RE ensures that most DR cases are detected, reducing the risk of missed diagnoses and vision loss. High PR minimizes false positives, avoiding unnecessary referrals and patient anxiety. SP helps correctly identify non-DR cases, reducing burden on healthcare resources. A balanced F1 indicates reliable detection in both positive and negative cases, which is crucial for clinical decision-making. Table 3 presents the classification performance obtained by proposed DR-FEDPAM model for diabetic retinopathy (DR) classification. AC, RE, F1, SP, and PR are the metrics used to determine

testing accuracy (AC). The MobileNet model achieves an accuracy of 98.36%, as observed from its training and testing accuracy curves across epochs. Fig. 5 b) illustrates the loss curve plotted against epochs, indicating that the loss decreases as the number of epochs increases. The proposed method produces accurate results with a relatively low loss of 1.6%. After both training and testing, the proposed network demonstrates strong overall performance.

## B. Comparative analysis

The effectiveness of each DL network was evaluated to verify that the proposed DR-FEDPAM model produces results with a high level of AC. In the comparative analysis, the baseline models AlexNet, ResNet, RegNet, and GoogleNet were implemented using standard publicly available architectures. All models, including the proposed DR-FEDPAM with MobileNet, were trained on the same DDR dataset. The

Table 3. Performance assessment of the proposed DR-FEDPAM model

Classes	AC	SP	PR	RE	F1
DR	97.90	95.27	97.02	96.33	96.48
No DR	98.82	96.12	95.70	94.21	97.89

performance. An overall accuracy of 98.36% was achieved by the proposed DR-FEDPAM model using the DDR dataset. Fig. 4 provides a representation of the DR-FEDPAM model's performance evaluation. In this figure, the proposed DR-FEDPAM model achieves 95.69%, 95.27%, 96.36%, and 97.18% for overall SP, RE, PR, and F1, respectively. High RE and F1 indicate strong DR detection with minimal missed cases. The balanced metrics demonstrate the model's reliability for clinical DR screening. In Fig. 5 a), the epochs on the x- and yaxes are shown along with a comparison of training and dataset was divided into 50% training, 30% testing, and 20% validation subsets to maintain uniformity. A batch size of 32 was used to train the models for 50 epochs using the AO with a learning rate of 0.001. Data augmentation techniques such as horizontal flipping, random cropping, and brightness adjustment were applied consistently across all models. These settings ensure that the performance comparison remains fair and reproducible under uniform experimental conditions. In Table 4, the proposed DR-FEDPAM model was compared with four classifiers: ResNet, AlexNet, RegNet, and GoogleNet. Several metrics

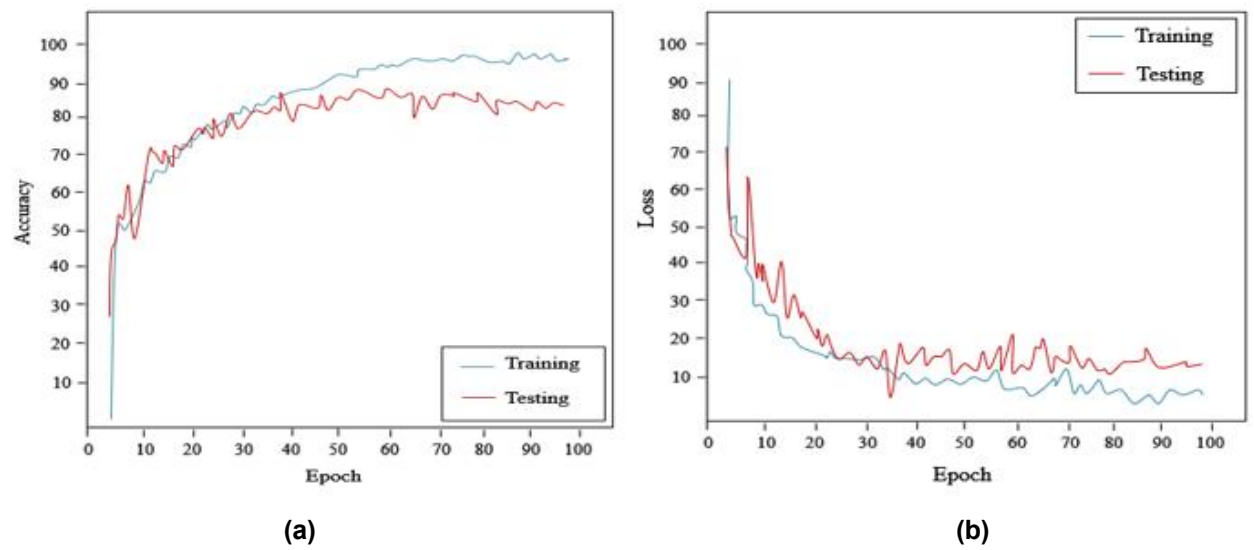


Fig. 5. Performance of the proposed DR-FEDPAM, (a) Accuracy and (b) loss graph

were used to evaluate each DL technique's performance, including F1, RE, PR, SP, and AC. The reported p-values from paired t-tests are all below 0.05, indicating that the performance improvements achieved by DR-FEDPAM are statistically significant. The proposed DR-FEDPAM model attained an overall accuracy of 98.36%. This study primarily focuses on binary classification, where DR-FEDPAM achieved a high accuracy of 98.05%, confirming its strong capability to distinguish between Normal and DR cases. Notably, during evaluation, the model also demonstrated promising performance in five-class classification, reaching an accuracy of 98.79%.

Although five-class classification is not part of the current DR-FEDPAM model, this result highlights its potential for future in multi-stage DR detection, enabling finer-grained classification of disease severity. Fig. 6 provides a graphical representation of the MobileNet comparative evaluation. The proposed MobileNet outperforms ResNet, AlexNet, RegNet, and GoogleNet by 4.1%, 3.1%, 3.9%, and 1.6%, respectively, in terms of overall accuracy. MobileNet also demonstrates superior performance in RE and F1, indicating strong detection capabilities with balanced PR. Its consistent lead across all metrics confirms its suitability for accurate and efficient DR classification.

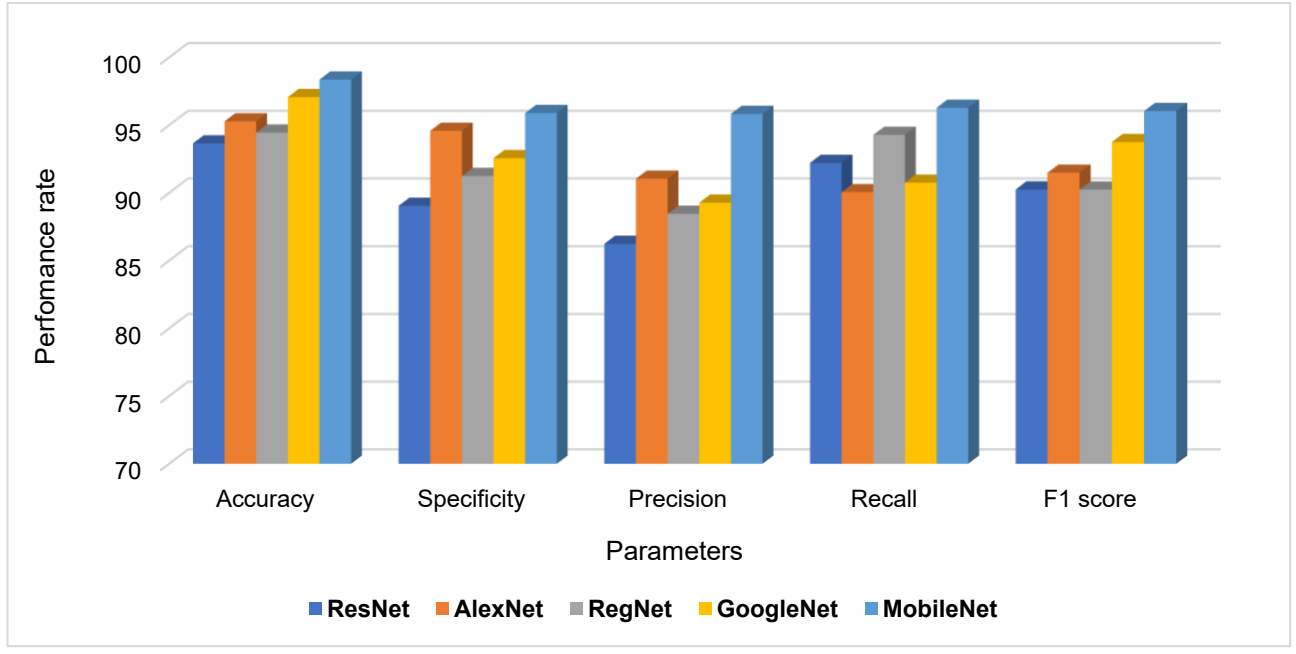


Fig. 6. A graphic representation of performance analysis for MobileNet

International License (CC BY-SA 4.0).

Table 4. Comparison between traditional DL networks and proposed the DR-FEDPAM model

Networks	AC	SP	PR	RE	F1	p-value	Binary classification	Five class classification
ResNet [36]	93.65	89.04	86.23	92.21	90.25	0.056	94.54	97.36
AlexNet [37]	95.28	94.58	91.04	90.05	91.48	0.070	95.76	96.12
RegNet [38]	94.45	91.24	88.45	94.28	90.24	0.066	96.24	97.88
GoogleNet [39]	97.07	92.56	89.27	90.75	93.75	0.054	97.21	98.34
MobileNet (proposed)	98.36	95.89	95.83	96.28	96.04	0.05	98.05	98.79

Table 5. Dataset comparison of the proposed DR-FEDPAM model

Dataset	AC	PR	RE
Kaggle DRD [40]	95.34	94.22	95.12
IDRiD [41]	93.58	91.54	93.73
MESSI-DOR [42]	91.20	93.45	90.32
DDR dataset (proposed)	98.36	95.83	96.28

Table 6. Performance comparison of the DR-FEDPAM model with and without pre-processing

Metrics	With pre-processing	Without pre- processing
AC	95.23	94.44
PR	92.10	91.12
SP	93.69	90.47
RE	91.73	89.55
F1	94.38	93.28

Table 5 presents the efficiency of the proposed DR-FEDPAM model for DR detection using different datasets. The existing datasets namely Kaggle DRD [40], IDRiD [41], and MESSI-DOR [42] exhibit relatively lower accuracy levels. The proposed DR-FEDPAM model achieved 98.36% AC, 95.83% PR, and 96.28% RE on the DDR dataset. The results emphasize that the proposed model attained better performance on the DDR dataset compared to the other datasets.

#### C. Ablation Study

An ablation study was conducted on the DR-FEDPAM model to evaluate the effect of preprocessing. The comparison includes configurations with and without preprocessing. A contrastive analysis of DR-FEDPAM with and without MeF and GaSF is presented in Table 6. Table 6 presents the comparative performance analysis of the DR-FEDPAM model under different configurations: with and without preprocessing. Applying preprocessing significantly improved model performance across all metrics, enhancing accuracy by

0.79% and F1 by 1.10%. Noise reduction and image quality enhancement through filtering contributed to improved feature extraction and classification accuracy.

## V. Discussion

The findings of this study highlight the effectiveness of the proposed DR-FEDPAM model in addressing two major challenges in DR detection: achieving high diagnostic accuracy while maintaining patient data privacy. By combining image preprocessing (Median Filter and Gaussian Star Filter) with a federated proximal averaging strategy, the model achieved an overall accuracy of 98.36%, which ranks among the reported for DR classification. demonstrates that lightweight architectures, when integrated with federated optimization, can provide robust feature extraction and reliable classification without requiring centralized data aggregation. The balanced performance across all key metrics precision.

Table 7. Comparing the accuracy of current models with DR-FEDPAM model

Authors	Approaches	AC	Parameters (Millions)	FLO Ps	Inference Time (ms)
Fayyaz, A.M et al [22]	AlexNet	93	15.5	3.1	25.3
Basheer, S. and Varghese, R.E., [23]	ResNet	96.5	10.3	4.3	14.6
Jabbar et al [25]	APSO	94	8.4	2.6	18.5
Proposed	DR-FEDPAM	98.36	7.8	1.7	13.9

recall, specificity, and F1 indicates that the model can effectively minimize both false negatives (reducing missed diagnoses) and false positives (preventing unnecessary referrals), which are critical for real-world clinical applications. Although DR-FEDPAM demonstrates strong performance, it is not without limitations. The experiments were conducted using publicly available datasets, which may not fully capture the diversity and complexity of real-world clinical environments. Additionally, while federated learning data privacy, it introduces potential communication overhead and synchronization delays when deployed across a large number of clients. Moreover, extreme variations in data quality or highly imbalanced class distributions could affect model generalization, warranting further investigation in future studies. Table 7 presents that during the testing stage, the experiment duration of images from the collected dataset was calculated to evaluate the accuracy of various methodologies. The classification accuracy for state-of-the-art percentages models determined and used to compare performance metrics. Compared to AlexNet, ResNet, and APSO, the DR-FEDPAM model improves overall accuracy by 5.44%, 1.89%, and 4.43%, respectively. The proposed network outperformed existing architectures in terms of overall performance. DR-FEDPAM achieves a balanced tradeoff with 7.8 million parameters, 1.7 GFLOPs, and an average inference time of 13.9 ms. This analysis demonstrates that the proposed method maintains practical computational efficiency suitable for real-time applications.

Despite its strong performance, the proposed model has several limitations. First, the study was conducted on publicly available datasets, which may not capture the full variability of clinical environments, such as imaging device differences, demographic variations, or low-quality scans. Second, while federated learning ensures privacy, it introduces communication overhead and synchronization challenges when scaled to a large number of clients. Third, like many deep learning systems, the model functions as a "black box," making it difficult for clinicians to interpret its decisions. This lack of explainability could limit trust and hinder adoption in

medical workflows. Addressing these issues through real-world validation, communication-efficient federated learning strategies, and the incorporation of explainable AI techniques such as Grad-CAM would further strengthen the model's clinical utility.

The implications of this study are significant for advancing Al-driven healthcare. By enabling privacypreserving collaborative learning, DR-FEDPAM aligns with regulations such as GDPR and HIPAA, making it a practical option for deployment in multi-institutional healthcare systems. The model's low computational demand and rapid inference time enable deployment not only in advanced hospitals but also in resourceconstrained settings, improving access to early DR screening in underserved regions. Furthermore, the scalability of the model suggests potential extensions to other imaging modalities, such as glaucoma or agerelated macular degeneration detection, thereby broadening its applicability. Recent studies have emphasized that federated learning is a promising paradigm for medical AI due to its ability to balance accuracy and privacy [23], [24]. Therefore, DR-FEDPAM not only advances the state of DR detection but also contributes to the broader vision of secure, collaborative, and globally applicable Al-assisted medical diagnostics.

#### VI. Conclusion

In this study, the DR-FEDPAM model was proposed for detecting DR. The input images were preprocessed and fed into a Federated Proximal Model. Federated learning enables multiple local models to train on different devices without sharing input images. After the local models process the data, the results are combined using a GFA model. Using parameters from all local models, the global model classifies images as either Normal or DR. The proposed MobileNet outperformed ResNet, AlexNet, RegNet, GoogleNet by 4.1%, 3.1%, 3.9%, and 1.6%, respectively, in terms of overall accuracy. As a result of the experiments, the proposed method achieved 98.36% accuracy, outperforming previous methods in classifying DR at its early stages. Compared to AlexNet. ResNet. and APSO, the DR-FEDPAM model improved overall accuracy by 5.44%, 1.89%, and

Journal of Electronics, Electromedical Engineering, and Medical Informatics

Homepage: jeeemi.org; Vol. 7, No. 4, October 2025, pp: 1259-1271 e-ISSN: 2656-8632

4.43%. One significant limitation of the DR-FEDPAM model is its reduced interpretability, which makes it challenging for clinicians to understand the reasoning behind its predictions. This lack of explainability may hinder clinical trust and adoption in real-world diagnostic workflows. To address this, future enhancements should incorporate explainable Al techniques such as Grad-CAM or attention maps to provide visual justification for the model's decisions. This would improve transparency, facilitate clinical validation, and support more informed medical decision-making.

#### **Acknowledgments**

The authors would like to express their heartfelt gratitude to the supervisor for their guidance and unwavering support throughout this study.

#### **Funding**

Not applicable.

## **Data Availability**

Data sharing is not applicable to this article, as no datasets were generated or analyzed during the current study.

#### **Author Contribution**

Gaya Nair P conceptualized and designed the study, conducted data collection, and participated in data analysis and interpretation. Lanitha B contributed to the development of the educational media, oversaw the implementation of the intervention, and contributed to manuscript writing and revisions. Gaya Nair P assisted with data analysis and interpretation and provided critical feedback on the manuscript. All authors reviewed and approved the final version of the manuscript and agreed to be responsible for all aspects of the work, ensuring its integrity and accuracy.

## **Declarations**

#### **Ethical Approval**

The research guide reviewed and ethically approved this manuscript for publication in this journal.

## **Consent for Publication**

Not applicable.

#### **Competing Interests**

The authors declare that there are no conflicts of interest regarding the publication of this paper

#### References

- [1] R. Vignesh, N. Muthukumaran and M. P. Austin, "Hybrid ResNet with bidirectional LSTM for eye disease classification with evaluation optimizers techniques," In 2023 International Conference on Inventive Computation Technologies (ICICT), pp. 1624-1630, 2023, doi: 10.1109/icict57646.2023.10134223
- [2] R. Priya and P. Aruna, "Diagnosis of diabetic retinopathy using machine learning techniques," *ICTACT Journal on soft computing*, vol. 3, no. 4, pp. 563-575, 2013, doi: 10.21917/ijsc.2013.0083
- [3] H.Y. Tsao, P.Y. Chan and E.C.Y. Su, "Predicting diabetic retinopathy and identifying interpretable biomedical features using machine learning algorithms," *BMC bioinformatics*, vol. 19, pp. 111-121, 2018, doi: 10.1186/s12859-018-2277-0
- [4] D. Das, S.K. Biswas and S. Bandyopadhyay, "A critical review on diagnosis of diabetic retinopathy using machine learning and deep learning," *Multimedia Tools and Applications*, vol. 81, no. 18, pp. 25613-25655, 2022, doi: 10.1007/s11042-022-12642-4
- [5] M.J. Hossain, M. Al-Mamun and M.R. Islam, "Diabetes mellitus, the fastest growing global public health concern: Early detection should be focused," *Health Science Reports*, vol. 7, no. 3, pp. e2004, 2024.
- [6] B.S. Mankar and N. Rout, "Automatic detection of diabetic retinopathy using morphological operation and machine learning," ABHIYANTRIKI Int. J. Eng. Technol, vol. 3, no. 5, pp. 12-19, 2016, doi: 10.1007/s11042-023-16813-9
- [7] F. Jeribi, T. Nazir, M. Nawaz, A. Javed, M. Alhameed and A. Tahir, "Recognition of diabetic retinopathy and macular edema using deep learning," *Medical & Biological Engineering & Computing*, pp. 1-15, 2024, doi: 10.1007/s11517-024-03105-z
- [8] J. Angel Sajani and A. Ahilan, "Classification of brain disease using deep learning with multimodality images," *J. Intell. Fuzzy Syst.* (Preprint), pp. 1-11, 2023, doi: 10.3233/jifs-230090
- [9] A. Ahilan, J. Angel Sajani, A. Jasmine Gnana Malar, B. Muthu Kumar, "Machine Learning-Based Brain Disease Classification Using EEG and MEG Signals," In International Conference on Frontiers of Intelligent Computing: Theory and Applications, pp. 487-498, 2023, doi: 10.1007/978-981-99-6702-5 40
- [10] B. Pradheep T Rajan and N. Muthukumaran, "Optimized CNN and adaptive RBFNN for channel estimation and hybrid precoding approaches for multi user millimeter wave massive MIMO," International Journal of Electronics, Published

- online, July 2024, doi: 10.1080/00207217.2024.2372060
- [11] R. Bala, A. Sharma and N. Goel, "Comparative Analysis of Diabetic Retinopathy Classification Approaches Using Machine Learning and Deep Learning Techniques," *Archives of Computational Methods in Engineering*, vol. 31, no. 2, 2024, doi: 10.1007/s11831-023-10002-5
- [12] Y. Suo, Z. He and Y. Liu, "Deep learning CS-ResNet-101 model for diabetic retinopathy classification," *Biomedical Signal Processing and Control*, vol. 97, pp. 106661, 2024, doi: 10.1016/j.bspc.2024.106661
- [13] I. Arias-Serrano, P.A. Velásquez-López, L.N. Avila-Briones, F.C. Laurido-Mora, F. Villalba-Meneses, A. Tirado-Espin, J. Cruz-Varela and D. Almeida-Galárraga, "Artificial intelligence based glaucoma and diabetic retinopathy detection using MATLAB—Retrained AlexNet convolutional neural network," F1000Research, vol. 12, pp. 14, 2024, doi: 10.12688/f1000research.122288.2
- [14] T.D. Nguyen, D.T. Le, J. Bum, S. Kim, S.J. Song and H. Choo, "Retinal disease diagnosis using deep learning on ultra-wide-field fundus images," *Diagnostics*, vol. 14, no. 1, pp. 105, 2024. doi: 10.3390/diagnostics14010105
- [15] B. Shi, X. Zhang, Z. Wang, J. Song, J. Han, Z. Zhang and T.T. Toe, "GoogLeNet-based Diabetic-retinopathy-detection," In 2022 14th International Conference on Advanced Computational Intelligence (ICACI), pp. 246-249, 2022, doi: 10.1109/icaci55529.2022.9837677
- [16] Cheepurupalli Raghuram, V. S. R. K. Raju Dandu and B. Jaison, "HYBRIDIZATION OF DILATED CNN WITH ATTENTION LINK NET FOR BRAIN CANCER CLASSIFICATION," International Journal of Data Science and Artificial Intelligence, vol. 02, no.02, pp. 35-42, 2024.
- [17] Jhansi Bharathi Madavarapu, "CAB-IDS: IoT-based Intrusion Detection using Bacteria Foraging Optimized BiGRU-CNN Network," *International Journal of Computer and Engineering Optimization*, vol. 01, no. 02, pp. 63-68, 2023.
- [18] D. Igrec, G. Golobich, and M. Urbanija, Design and Optimization of Affordable Embedded Medical Devices for Resource-Constrained Settings, 2025.
- [19] G. Kaissis, A. Ziller, J. Passerat-Palmbach, T. Ryffel, D. Usynin, A. Trask, I. Lima Jr, J. Mancuso, F. Jungmann, M.M. Steinborn and A. Saleh, "End-to-end privacy preserving deep learning on multi-institutional medical imaging," *Nature Machine Intelligence*, 3(6), pp. 473-484, 2021, doi: 10.1038/s42256-021-00337-8
- [20] C. Lahmar and A. Idri, "Classifying Diabetic Retinopathy using CNN and Machine Learning," *In Bioimaging*, pp. 52-62, 2022, doi: 10.5220/0010851500003123

- [21] S. Dasari, B. Poonguzhali and M.S. Rayudu, "An efficient machine learning approach for retinopathy classification diabetic of stages," Indonesian Journal Electrical of Engineering and Computer Science, vol. 30, no. 1, pp. 81-88, 2023, doi: 10.11591/jieecs.v30.i1.pp81-88
- [22] A.M. Fayyaz, M.I. Sharif, S. Azam, A. Karim and J. El-Den, "Analysis of diabetic retinopathy (DR) based on the deep learning," *Information*, vol. 14, no. 1, pp. 30, 2023, doi: 10.3390/info14010030
- [23] S. Basheer and R.E. Varghese, "Estimation of diabetic retinopathy using deep learning," *In AIP Conference Proceedings*, vol. 3059, no. 1, 2024, doi: 10.1063/5.0194492
- [24] V. Sapra, L. Sapra, A. Bhardwaj, A. Almogren, S. Bharany, A. Ur Rehman and K. Ouahada, "Diabetic Retinopathy Detection Using Deep Learning with Optimized Feature Selection," *Traitement du Signal*, pp. 41, no. 2, 2024, doi: 10.18280/ts.410219
- [25] A. Jabbar, H.B. Liaqat, A. Akram, M.U. Sana, I.D. Azpíroz, I.D.L.T. Diez and I. Ashraf, "A Lesion-Based Diabetic Retinopathy Detection Through Hybrid Deep Learning Model," *IEEE Access*, 2024, doi: 10.1109/access.2024.3373467
- [26] R. Chaudhuri and S. Deb, "Precise lesion analysis to detect diabetic retinopathy using Generative Adversarial Network (GAN) and Mask-RCNN," Procedia Computer Science, vol. 235, pp. 520-529, 2024, doi: 10.1016/j.procs.2024.04.051
- [27] A.M. Mutawa, K. Al-Sabti, S. Raizada and S. Sruthi, "A Deep Learning Model for Detecting Diabetic Retinopathy Stages with Discrete Wavelet Transform," *Applied Sciences*, vol. 14, no. 11, pp. 4428, 2024, doi: 10.3390/app14114428
- [28] D.A. Da Rocha, F.M.F. Ferreira, and Z.M.A. Peixoto, "Diabetic retinopathy classification using VGG16 neural network," *Research on Biomedical Engineering*, vol. 38, no. 2, pp.761-772, 2022, doi: 10.1007/s42600-022-00200-8
- [29] B. Ramasubramanian and S. Selvaperumal, "A comprehensive review on various preprocessing methods in detecting diabetic retinopathy," In 2016 international conference on communication and signal processing (ICCSP), pp. 0642-0646, 2016, doi: 10.1109/iccsp.2016.7754220
- [30] H. Avcı and J. Karakaya, "A novel medical image enhancement algorithm for breast cancer detection on mammography images using machine learning," *Diagnostics*, vol. 13, no. 3, pp. 348, 2023, doi: 10.3390/diagnostics13030348
- [31] K. Malathi and R. Nedunchelian, "An Efficient Method to Detect Diabetic Retinopathy Using Gaussian-Bilateral and Haar Filters with Threshold Based Image Segmentation,"

- Research Journal of Applied Sciences, Engineering and Technology, vol. 8, no. 11, pp.1389-1395, 2014, doi: 10.19026/rjaset.8.1112
- [32] K. Kumar and B.T. Chakkaravarthy, "Contrast Enhancement and Noise Reduction Through Synthesizing Gaussian Filter, CLAHE and HE Algorithm for Image Preprocessing," In 2025 International Conference on Emerging **Technologies** in Engineering **Applications** (ICETEA). 2025, pp. 1-5, doi: 10.1109/icetea64585.2025.11100055
- [33] A. APPATHURAI, A. S. I. TINU and M. NARAYANAPERUMAL, "MEG AND PET IMAGES-BASED BRAIN TUMOR DETECTION USING KAPUR'S OTSU SEGMENTATION AND SOOTY-OPTIMIZED MOBILENET CLASSIFICATION," REVUE ROUMAINE DES SCIENCES TECHNIQUES—SÉRIE ÉLECTROTECHNIQUE ET ÉNERGÉTIQUE, vol. 69, no. 3, pp. 363-368, 2024, doi: 10.59277/rrst-ee.2024.69.3.18.
- [34] T. Zhou, Z. Lin, J. Zhang, and D.H. Tsang, "Understanding and improving model averaging in federated learning on heterogeneous data," *IEEE Transactions on Mobile Computing*, vol. 23, no. 12, pp.12131-12145, 2024, doi: 10.1109/tmc.2024.3406554
- [35] A. Bilal, M. Shafiq, W.J. Obidallah, Y.A. Alduraywish, A. Tahir and H. Long, "Quantum chimp-enanced SqueezeNet for precise diabetic retinopathy classification," *Scientific Reports*, vol. 15, no. 1, pp. 12890, 2025, doi: 10.1038/s41598-025-97686-w
- [36] R.S. Rajkumar and A.G. Selvarani, "Diabetic Retinopathy Diagnosis Using ResNet with Fuzzy Rough C-Means Clustering," *Computer Systems Science & Engineering*, vol. 42, no. 2, 2022, doi: 10.32604/csse.2022.021909
- [37] S. Balaji and B. Karthik, "A Context for Effective Prediction and Classification of Diabetic Retinopathy Disease using Deep Ensemble AlexNet & LeNet Classifier," In 2024 11th International Conference on Computing for Sustainable Global Development (INDIACom), pp. 414-421, 2024, doi: 10.23919/indiacom61295.2024.10498405
- [38] S. Chaurasiya, N. Singh and A. Singh, "Mobile-based diabetic retinopathy detection and classification using TinyML," In Advances in Science, Engineering and Technology, pp. 398-404, 2025, doi: 10.1201/9781003641544-73
- [39] B. Shi, X. Zhang, Z. Wang, J. Song, J. Han, Z. Zhang and T.T. Toe, "GoogLeNet-based Diabetic-retinopathy-detection," In 2022 14th International Conference on Advanced Computational Intelligence (ICACI), pp. 246-249, 2022, doi: 10.1109/icaci55529.2022.9837677

- [40] M.T. Hagos and S. Kant, "Transfer learning based detection of diabetic retinopathy from small dataset," arXiv preprint arXiv:1905.07203, 2019.
- [41] P. Porwal, S. Pachade, R. Kamble, M. Kokare, G. Deshmukh, V. Sahasrabuddhe and F. Meriaudeau, "Indian diabetic retinopathy image dataset (IDRiD): a database for diabetic retinopathy screening research," *Data*, vol. 3, no. 3, pp. 25, 2018, doi: 10.3390/data3030025
- [42] L. Giancardo, T.P. Karnowski, K.W. Tobin, F. Meriaudeau and E. Chaum, "Validation of microaneurysm-based diabetic retinopathy screening across retina fundus datasets,' In Proceedings of the 26th IEEE International Symposium on Computer-Based Medical 125-130, 2013. Systems, pp. doi: 10.1109/cbms.2013.6627776

#### **Author Biography**



Gaya Nair P is currently a Research Scholar in the Department of Computer Science and Engineering at Karpagam Academy of Higher Education, Coimbatore, Tamil Nadu. She completed her M.Tech in Computer Science and Engineering from Nehru College of Engineering

and Technology, Pampady, Thrissur, Kerala, and her B.Tech in Information Technology from Government Engineering College, Palakkad, Kerala. She has more than 10 years of teaching experience in various prestigious engineering colleges in Kerala and has been working as an Assistant Professor in the Department of Computer Science and Engineering at MES Engineering College, Kuttippuram, Kerala, for the past two years. Her research interests include Machine Learning and Image Processing.



Lanitha B received her Doctoral degree in Information and Communication Engineering from Anna University, Chennai. She has 16 years of teaching experience in reputed engineering colleges and is currently working as an Associate Professor at Karpagam Academy of

Higher Education, Coimbatore. Her research interests include Cloud Computing, Machine Learning, Deep Learning, Big Data, and Software Engineering. She has filed two patents and authored two books. She is a member of IEEE, NCSSS, and IAENG. She has published papers in reputed conferences and journals, including Springer, IEEE, and the Journal of Nanomaterials.